Upconversion

International Edition: DOI: 10.1002/anie.201711606
German Edition: DOI: 10.1002/ange.201711606

Precisely Tailoring Upconversion Dynamics via Energy Migration in Core–Shell Nanostructures

Jing Zuo[+], Dapeng Sun[+], Langping Tu[+], Yanni Wu, Yinghui Cao, Bin Xue, Youlin Zhang, Yulei Chang, Xiaomin Liu, Xianggui Kong, Wybren Jan Buma, Evert Jan Meijer,* and Hong Zhang**

Abstract: *Upconversion emission dynamics have long been believed to be determined by the activator and its interaction with neighboring sensitizers. Herein this assumption is, however, shown to be invalid for nanostructures. We demonstrate that excitation energy migration greatly affects upconversion emission dynamics. "Dopant ions' spatial separation" nanostructures are designed as model systems and the intimate link between the random nature of energy migration and upconversion emission time behavior is unraveled by theoretical modelling and confirmed spectroscopically. Based on this new fundamental insight, we have successfully realized fine control of upconversion emission time behavior (either rise or decay process) by tuning the energy migration paths in various specifically designed nanostructures. This result is significant for applications of this type of materials in super resolution spectroscopy, high-density data storage, anti-counterfeiting, and biological imaging.*

Lanthanide (Ln) ions doped upconversion (UC) materials have attracted extensive attention owing to their potential applications in a large variety of fields, for example, display,[1] biology,[2] anti-counterfeiting,[3] and solar cells.[4] Recent advances in upconversion emission applications rely more and more on precisely engineering the material structure on nanometer scale, in which energy migration behavior plays a key role. So far, most of the related investigations have focused on steady-state effects of energy migration.[5] That is, excited states could randomly "walk", thus making the long-range energy transport (more than several nanometers) between Ln^{3+} ions possible. However, the lack of a detailed microscopic picture of UC mechanism in such structures, especially the ambiguous recognition of the energy migration dynamics and its effect on the time behavior of UC emission, remains a major bottleneck for further development of these structures.

Based on traditional understanding, energy migration among sensitizers is always neglected in UC dynamics treatment. In that case, although UC emission involves complex interactions between multiple Ln^{3+} ions, its dynamics are solely determined by the energy transfer processes within one activator–sensitizer pair (Figure 1 a).[6] Despite some discussion of this assumption,[7] there is no direct evidence of the effect of the sensitizer-to-sensitizer energy migration on UC dynamics.

This unsatisfactory situation is primarily due to the lack of appropriate material systems. Indeed, even in the traditional sensitizer–activator co-doping materials, energy migration still plays an important role in their UC process.[7a] However, its effect is difficult to evaluate as the energy migration process is indistinguishable from energy transfer between sensitizers and activators. In our opinion, this dilemma can be solved by introducing a smart nanosystem termed "dopant ions' spatial separation" (DISS) nanostructure.[5k] By locating sensitizers and activators into different regions of a single nanoparticle, the three basic processes of UC (i.e. light absorption, energy migration, and UC emission) can be well separated (Figure 1 b). Therefore, the role of energy migration in UC dynamics could be quantitatively determined by 1) tuning the migration layer thickness or 2) varying the dopant concentration of the ions as energy carriers in the migration layer. Secondly, traditional treatment of the UC mechanism based on simultaneous rate equations is not able to describe properly the actual energy migration processes, because it provides only an averaged macroscopic statistical result. Therefore, we set up a time-correlated Monte Carlo simulation model to fill the gap (Figure S1–S7, Table S1–S3, in the Supporting Information). Compared with previous approaches,[5e,7a,8] our model is capable of monitoring UC dynamics from the level of multiple ion-to-ion interactions,

[*] Dr. J. Zuo,[+] Dr. L. P. Tu,[+] Dr. B. Xue, Dr. Y. L. Zhang, Dr. Y. L. Chang, Prof. X. M. Liu, Prof. X. G. Kong, Prof. H. Zhang
State Key Laboratory of Luminescence and Applications, Changchun Institute of Optics, Fine Mechanics and Physics, Chinese Academy of Sciences
Changchun 130033 (China)
E-mail: xgkong14@ciomp.ac.cn
Dr. J. Zuo,[+]
University of the Chinese Academy of Sciences
Beijing 100049 (China)
Dr. J. Zuo[+] Dr. D. P. Sun,[+] Dr. Y. N. Wu, Prof. W. J. Buma, Prof. E. J. Meijer, Prof. H. Zhang
Van't Hoff Institute for Molecular Sciences, University of Amsterdam
Science Park 904, 1098 XH Amsterdam (The Netherlands)
E-mail: E.J.Meijer@uva.nl
H.Zhang@uva.nl
Dr. Y. H. Cao
College of Computer Science and Technology, Jilin University
2699 Qianjin Street, Changchun, Jilin 130021 (China)
[+] These authors contributed equally to this work.
Supporting information and the ORCID identification number(s) for the author(s) of this article can be found under: https://doi.org/10.1002/anie.201711606.

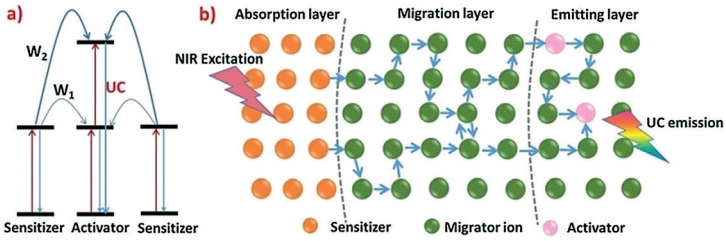

Figure 1. Schematic diagram of a) the traditional UC mechanism which relies on the monomer (sensitizer) to monomer (activator) sequential energy transfer interactions, and b) the UC process in the DISS nanostructure, in which the three basic processes: photon absorption, energy migration, and UC emission are spatially separated.

yielding a more comprehensive vision without restriction of the distribution of Ln^{3+} ions in the nanostructure.

Combining the experimental and simulation results, we find that despite each step of the energy migration (e.g. $Yb^{3+}\rightarrow Yb^{3+}$) only costs a relatively short time (around microseconds), its randomly walking nature significantly prolongs the migration time up to several hundred microseconds. This result tells us that the conventional understanding of the UC mechanisms is incomplete and in some nanostructures it might be misleading by ignoring the actual energy-migration process. More importantly, by precisely tuning energy migration paths in a DISS nanostructure, either the rise or decay of UC emission dynamic traces can be quantitatively tailored in a wide range. Our study thus not only offers a new distinct microscopic picture on how energy migration affects UC and the temporal characteristics of UC emission, but is also an excellent starting point for the rational design of novel functional and efficient UC nanostructures.

We prepared a DISS nanostructure: YbEr@Yb@ YbNd (short for $NaYF_4$: 20% Yb, 2% Er @$NaYF_4$: 20% Yb @$NaYF_4$: 10% Nd, 20% Yb) to explore the temporal effect of energy migration. The pure hexagonal phase of the nanoparticles was confirmed by the X-ray powder diffraction (Figure S8). The uniformed sizes (or thickness) of the core and each shell were verified to be approximately 25.0 nm, 2.8 nm, 3.0 nm, respectively (Figure S9). To perform spectroscopic studies, a binary pulse excitation setup was designed, in which the interval (Δt) between a 800 nm and a 980 nm nanosecond pulse is tunable from −200 μs to 1000 μs (Figure 2a). Typically, 980 nm laser excites Yb^{3+} ions all over the whole nanoparticle, whereas 800 nm only excites Nd^{3+} ions located in the outer layer (Figure 2b). The UC emission comes from 1) 980 nm excitation, 2) 800 nm excitation, and 3) 980 nm and 800 nm co-excitation. Clearly, the first two parts (1 and 2) are Δt independent, and part (3) depends on Δt. Strikingly, the strongest UC emission occurs not at $\Delta t = 0$, but at the point when the 980 nm pulse is approximately 200 μs behind the 800 nm pulse (Figure 2c). Furthermore, since the time constant of $Nd^{3+}\rightarrow Yb^{3+}$ energy transfer is very short (ca. 20 μs, Figure S10), the approximately 200 μs time delay should be mainly attributed to the additional $Yb^{3+}\rightarrow Yb^{3+}$ energy migration time under the 800 nm excitation. Significance of this result is that: 1) it is the first acquisition in real time of energy migration contribution to UC emission, and 2) it confirms that the energy migration temporal effect is non-negligible. This result is consistent with the prediction of Monte Carlo simulation. In $NaYF_4$:20% Yb sublattice, despite each step of $Yb^{3+}\rightarrow Yb^{3+}$ energy migration only takes about 1.7 μs (Figure S5), and even if the migration distance is just a few nanometers, the time delay for UC will still be several hundred microseconds because 1) the random walk nature of energy migration, and 2) the non-linear nature of UC emission (Figure S11). To validate this assumption, two types of DISS nanostructure are designed to tune the rise and decay of UC dynamics, respectively.

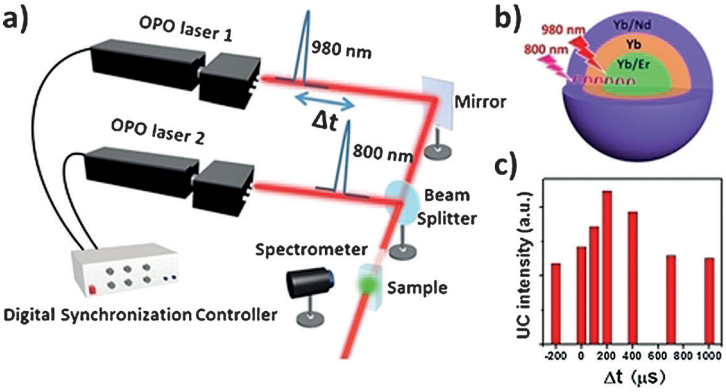

Figure 2. a) Schematic diagram of the experimental setup for binary pulsed (800 nm and 980 nm) excitation. b) The YbEr@Yb@YbNd UC nanostructure used in the binary pulsed excitation experiment. c) Time-gap (difference between 800 and 980 nm pulses) dependent UC emission intensity of the YbEr@Yb@YbNd nanoparticles (integrated from 500 nm to 700 nm).

To quantitatively tune the rise of the time trace of UC emission, the DISS nanostructure characterized with spatially separated absorption (sensitizer) and emission (activator) regions is suggested. As an example, the 800 nm excited YbEr@Yb@Nd core/shell/shell nanostructure (short for $NaYF_4$: 20% Yb, 2% Er@$NaLuF_4$: 20% Yb@$NaYF_4$:20%Nd) is employed. The UC emission of this structure relies fully on the $Yb^{3+}\rightarrow Yb^{3+}$ energy transfer to transport the absorbed energy from the outer layer to the core area (Figure 3a). The pure hexagonal phase and narrow size distribution of nanoparticle are confirmed by Fourier-transform diffraction pattern and TEM images (Figures 3b and Figure S12). Besides, the core/shell/shell structure is directly confirmed by distinguishing the lighter lanthanide element (Y, brighter parts) and the heavier one (Lu, darker parts) in the TEM image (Figures 3b). Clearly, because of the non-negligible $Yb^{3+}\rightarrow Yb^{3+}$ energy migration time (ca. 1.7 μs per step) in the $NaLuF_4$: 20% Yb^{3+} middle layer, the required time of Er^{3+} receiving the migrated energy can be well controlled by the layer thickness, appearing as a tunable rise of UC luminescence time trace. Indeed, increasing the

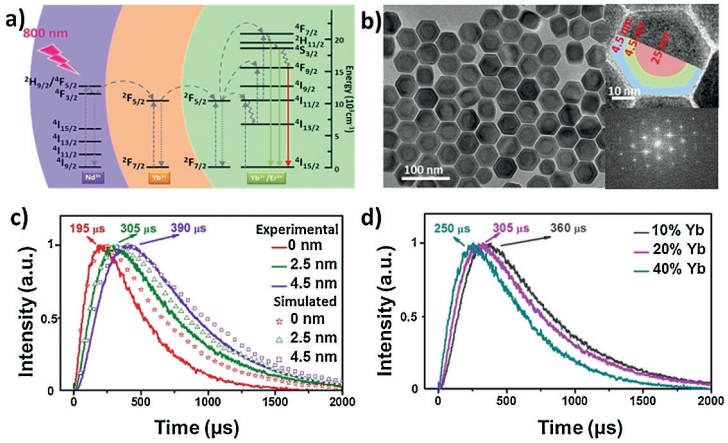

Figure 3. a) Schematic representation of the UC process in the YbEr@Yb@Nd DISS nanostructure under 800 nm excitation. b) Typical TEM image (left), expanded area of TEM image (upper right) and Fourier-transform diffraction patterns (lower right) of the YbEr@Yb@Nd nanostructure. c) The energy migration distance (i.e. middle layer thickness) dependent 540 nm UC emission traces. Solid traces are the experimental results and dotted traces are the simulation results. d) The influence of Yb^{3+} dopant concentration in the middle layer (ca. 2.5 nm) on the 540 nm UC emission traces.

thickness of middle layer from 0 to about 4.5 nm results in prolongation of rise of around 540 nm UC emission ($^4S_{3/2}$ energy state) from 195 to 390 μs (Figure 3c, solid traces). Similar result has also been observed for $^4F_{9/2}$ energy state (ca. 650 nm UC emission), which varies from 383 to 607 μs (Figure S13).

Note that without the long-distance energy migration, such a large time span modulation of the rise is hardly achieved in traditional Yb^{3+}/Er^{3+} co-doping systems.[7e,9] Importantly, such a tuning effect is well predicted by our simulation model (Figure 3c, dotted traces). The only exception is the sample without a middle layer (the red solid and dotted traces in Figure 3c). The deviation most probably comes from the model simplification, which ignores the efficient $Er^{3+}\rightarrow Nd^{3+}$ energy quenching process.[5f] In addition, the influence of Yb^{3+} dopant concertation on energy migration dynamics has been studied. As shown in Figure 3d, the migration time will decrease as the Yb^{3+} dopant concertation increases. The reason is discussed in details in Supporting Information (Figure S14 and Table S4). Furthermore, to verify the universality of our approach, another DISS nanostructure, that is, $NaYF_4$: 20% Yb, 2% Er @$NaYF_4$: 20% Yb @$NaYF_4$: 10% Nd, 20%Yb has been tested, and similar results were obtained (Figure S15).

Next we turn to tune the decay of time-resolved UC emission in a wide range, which is not only required for practical applications,[10] but also very important for an in-depth understanding of the UC mechanism.[11] Up to now, modulation approach was almost exclusively addressed by changing the depopulation rate of the activator emitting energy level, such as surface modification, Ln^{3+} dopant concentration manipulation, plasmonic effect and introducing extra energy transfer channels.[11a,12] However, all these approaches usually bring along limitations including 1) a limited tuning range, and 2) UC efficiency reduction. Herein, we propose a novel strategy, that is, utilizing the energy migration process in DISS nanostructures characterized with partly overlapped sensitizer and activator regions. As an example, a series of YbEr@Yb core/active shell DISS nanostructures (short for $NaYF_4$: 20% Yb, 2% Er@$NaYF_4$: 20% Yb) were synthesized. The high quality of the nanostructures is confirmed by SEM images in Supporting Information (Figure S16).

As shown in Figure 4a,b, the UC processes in this DISS nanostructure can be roughly divided into three parts. In part I, Yb^{3+} and Er^{3+} are co-doped, therefore its UC emission dynamics presents as a relatively sharp rise due to the minimal energy migration time (black curve in Figure 4b). On the contrary, for parts II and III, the spatially separated Yb^{3+} and Er^{3+} require the excitation energy to migrate with more time to achieve UC emission, which leads to 1) slower rises, and 2) relatively low UC efficiency due to the energy loss in the migration process (the green line and blue line in Figure 4b). Notably, the UC emission time trace is a profile of contributions of all the three parts, thus it makes the decay longer than any of the individual parts (Figure 4b). As indicated in Figure 4c, the UC emission (ca. 540 nm) decay lifetime (the required time for transient emission intensity to decay from its maximum value to its 1/e value) could be tuned over a wide range from 139 to 648 μs by varying the active shell thickness from 0 to 15 nm. Meanwhile, the rises change little (from 36 to 144 μs, Figure S17) because they are all dominated by the common part I. The significance of the results is that 1) it breaks through the limitation of the traditional co-doping system.

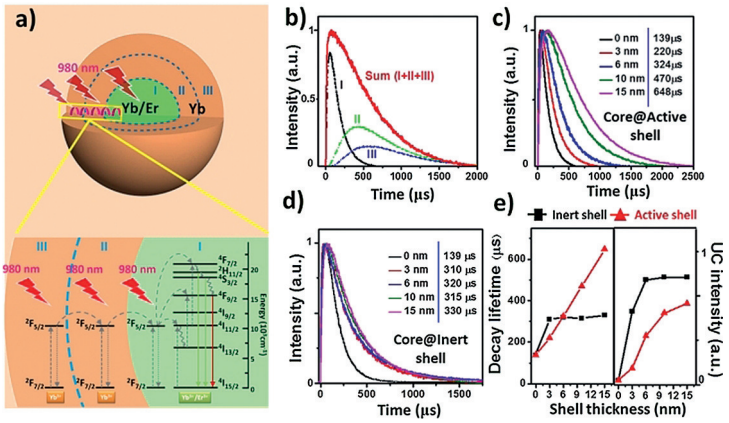

Figure 4. a) Schematic representation of UC processes in YbEr@Yb core/active shell nanostructure under the 980 nm excitation. b) Schematic representation of UC emission trace of YbEr@Yb nanostructure (red line) and its equivalent emission origins (black trace from part I, green trace from part II, and blue trace from part III). Shell thickness dependent 540 nm UC emission traces of the c) core/active shell structures and d) core/inert shell structures. e) 540 nm decay lifetimes (left) and 540 nm UC emission intensities (right) of core/inert shell structures (black curve) and core/active shell structures (red curve).

Without the assistance of energy migration in the shell, YbEr@Y core/inert shell structures (short for $NaYF_4$: 20% Yb, 2% Er@$NaYF_4$), as a control, offer a relatively narrow tuning range (from 139 to 330 μs) via eliminating the surface quenching effect (Figure 4d). 2) It guides us to reconsider the relationship between UC efficiency and decay lifetime. Based on the empirical views developed from sensitizer-activator co-doping systems, the longer UC emission decay lifetime is often related to a higher UC efficiency due to the reduction of nonradiative relaxation rate. This view is, however, not always valid to DISS nanostructures. As indicated in Figure 4e, compared with YbEr@Y nanostructure, the YbEr@Yb DISS nanostructure exhibits a relatively long decay lifetime but a relatively low UC efficiency when the shell thickness is over 6 nm. This "abnormal" phenomenon can be explained by 1) the energy migration effect of the active shell (prolonging the decay lifetime) and 2) the efficient energy back-transfer from core to active shell (decreasing the UC efficiency) (Figure S18,19 and Table S5). It is quite gratifying to notice that the "abnormal" phenomenon is well predicted by our Monte Carlo simulations (Figure S20 and Table S6).

In summary, long-standing puzzle of the intimate link between excitation energy migration and UC emission dynamics is unraveled through theoretical modeling and spectroscopic experiments of specifically designed "dopant ions' spatial separation" nanostructure. The contribution of excitation migration to the UC emission dynamics is demonstrated to be significant as a result of the accumulative effect of multiple-step random walks of the excitation energy. Based on this improved understanding, we propose and demonstrate a convenient and effective approach for tailoring UC dynamics (either the rise or decay) through tuning the excitation energy migration paths in "dopant ions' spatial separation" nanostructures. Our study paves the way for application-optimized design of novel functional UC nanostructures and even to improve the UC emission efficiency.

Acknowledgements

This work was financially supported by NSF of China (11374297, 61575194, 11674316, 11504371, 11471278 and 11604331), Project of Science and Technology Agency, Jilin Province (20170520113JH, 20170520112JH and 20170519002JH), Joint research program between CAS of China and KNAW of the Netherlands, European Union MSCA-ITN-ETN Action program, ISPIC, under grant Nr. 675743, Netherlands Organisation for Scientific Research in the framework of the Fund New Chemical Innovation under grant Nr.731.015.206, European COST Action (CM1403), John van Geuns Fellowship under auspices of the HRSMC and Innovation project of State Key Laboratory of Luminescence and Applications of China. The work of Dr. D. P. Sun is supported by the research program of the "Stichting voor Fundamenteel Onderzoek der Materie (FOM)", which is financially supported by the 'Nederlandse Organisatie voor Wetenschappelijk Onderzoek (NWO).

Conflict of interest

The authors declare no conflict of interest.

Keywords: core–shell nanostructures · energy migration · lanthanides · luminescence dynamics · Monte Carlo simulation · upconversion nanocrystals

How to cite: *Angew. Chem. Int. Ed.* **2018**, *57*, 3054–3058
Angew. Chem. **2018**, *130*, 3108–3112

[1] a) R. Deng, F. Qin, R. Chen, W. Huang, M. Hong, X. Liu, *Nat. Nanotechnol.* **2015**, *10*, 237–242; b) C. Zhang, L. Yang, J. Zhao, B. Liu, M. Y. Han, Z. Zhang, *Angew. Chem. Int. Ed.* **2015**, *54*, 11531–11535; *Angew. Chem.* **2015**, *127*, 11693–11697; c) L. Wang, Y. Li, *Nano Lett.* **2006**, *6*, 1645–1649.

[2] a) Q. Su, W. Feng, D. Yang, F. Li, *Acc. Chem. Res.* **2017**, *50*, 32–40; b) N. M. Idris, M. K. Gnanasammandhan, J. Zhang, P. C. Ho, R. Mahendran, Y. Zhang, *Nat. Med.* **2012**, *18*, 1580–1585; c) D. Wang, B. Xue, X. Kong, L. Tu, X. Liu, Y. Zhang, Y. Chang, Y. Luo, H. Zhao, H. Zhang, *Nanoscale* **2015**, *7*, 190–197; d) C. Drees, A. N. Raj, R. Kurre, K. B. Busch, M. Haase, J. Piehler, *Angew. Chem. Int. Ed.* **2016**, *55*, 11668–11672; *Angew. Chem.* **2016**, *128*, 11840–11845; e) X. Li, Z. Guo, T. Zhao, Y. Lu, L. Zhou, D. Zhao, F. Zhang, *Angew. Chem. Int. Ed.* **2016**, *55*, 2464–2469; *Angew. Chem.* **2016**, *128*, 2510–2515; f) Y. Yang, Q. Shao, R. Deng, C. Wang, X. Teng, K. Cheng, Z. Cheng, L. Huang, Z. Liu, X. Liu, B. Xing, *Angew. Chem. Int. Ed.* **2012**, *51*, 3125–3129; *Angew. Chem.* **2012**, *124*, 3179–3183; g) L. Cheng, K. Yang, Y. Li, J. Chen, C. Wang, M. Shao, S. T. Lee, Z. Liu, *Angew. Chem. Int. Ed.* **2011**, *50*, 7385–7390; *Angew. Chem.* **2011**, *123*, 7523–7528; h) S. H. Nam, Y. M. Bae, Y. I. Park, J. H. Kim, H. M. Kim, J. S. Choi, K. T. Lee, T. Hyeon, Y. D. Suh, *Angew. Chem. Int. Ed.* **2011**, *50*, 6093–6097; *Angew. Chem.* **2011**, *123*, 6217–6221; i) L. Xia, X. Kong, X. Liu, L. Tu, Y. Zhang, Y. Chang, K. Liu, D. Shen, H. Zhao, H. Zhang, *Biomaterials* **2014**, *35*, 4146–4156; j) S. Li, L. Xu, W. Ma, X. Wu, M. Sun, H. Kuang, L. Wang, N. A. Kotov, C. Xu, *J. Am. Chem. Soc.* **2016**, *138*, 306–312; k) X. Yang, H. Xie, E. Alonas, Y. Liu, X. Chen, P. J. Santangelo, Q. Ren, P. Xi, D. Jin, *Light: Sci. Appl.* **2016**, *5*, e16134.

[3] a) X. Liu, Y. Wang, X. Li, Z. Yi, R. Deng, L. Liang, X. Xie, D. T. B. Loong, S. Song, D. Fan, A. H. All, H. Zhang, L. Huang, X. Liu, *Nat. Commun.* **2017**, https://doi.org/10.1038/s41467-017-00916-00917; b) Y. Zhang, L. Zhang, R. Deng, J. Tian, Y. Zong, D. Jin, X. Liu, *J. Am. Chem. Soc.* **2014**, *136*, 4893–4896; c) H. Liu, M. K. G. Jayakumar, K. Huang, Z. Wang, X. Zheng, H. Agren, Y. Zhang, *Nanoscale* **2017**, *9*, 1676–1686; d) K. Huang, N. M. Idris, Y. Zhang, *Small* **2016**, *12*, 836–852; e) J. Zuo, Q. Li, B. Xue, C. Li, Y. Chang, Y. Zhang, X. Liu, L. Tu, H. Zhang, X. Kong, *Nanoscale* **2017**, *9*, 7941–7946.

[4] a) M. He, X. Pang, X. Liu, B. Jiang, Y. He, H. Snaith, Z. Lin, *Angew. Chem. Int. Ed.* **2016**, *55*, 4280–4284; *Angew. Chem.* **2016**, *128*, 4352–4356; b) X. Huang, S. Han, W. Huang, X. Liu, *Chem. Soc. Rev.* **2013**, *42*, 173–201; c) W. Zou, C. Visser, J. A. Maduro, M. S. Pshenichnikov, J. C. Hummelen, *Nat. Photonics* **2012**, *6*, 560–564.

[5] a) X. Li, X. Liu, D. M. Chevrier, X. Qin, X. Xie, S. Song, H. Zhang, P. Zhang, X. Liu, *Angew. Chem. Int. Ed.* **2015**, *54*, 13312–13317; *Angew. Chem.* **2015**, *127*, 13510–13515; b) X. Chen, L. Jin, T. Sun, W. Kong, S. F. Yu, F. Wang, *Small* **2017**, https://doi.org/10.1002/smll.201701479; c) N. J. J. Johnson, S. He, S. Diao, E. M. Chan, H. Dai, A. Almutairi, *J. Am. Chem. Soc.* **2017**, *139*, 3275–3282; d) X. Chen, L. Jin, W. Kong, T. Sun, W. Zhang, X. Liu, J. Fan, S. F. Yu, F. Wang, *Nat. Commun.* **2016**, *7*, 10304; e) Y. Zhong, I. Rostami, Z. Wang, H. Dai, Z. Hu, *Adv. Mater.* **2015**, *27*, 6418–6422; f) Y. Zhong, G. Tian, Z. Gu, Y. Yang, L. Gu, Y.

Zhao, Y. Ma, J. Yao, *Adv. Mater.* **2014**, *26*, 2831 – 2837; g) J. Wang, R. Deng, M. A. MacDonald, B. Chen, J. Yuan, F. Wang, D. Chi, T. S. A. Hor, P. Zhang, G. Liu, Y. Han, X. Liu, *Nat. Mater.* **2014**, *13*, 157 – 162; h) F. Wang, R. Deng, J. Wang, Q. Wang, Y. Han, H. Zhu, X. Chen, X. Liu, *Nat. Mater.* **2011**, *10*, 968 – 973; i) Q. Su, S. Han, X. Xie, H. Zhu, H. Chen, C. K. Chen, R.-S. Liu, X. Chen, F. Wang, X. Liu, *J. Am. Chem. Soc.* **2012**, *134*, 20849 – 20857; j) M. Ding, D. Chen, D. Ma, J. Dai, Y. Li, Z. Ji, *J. Mater. Chem. C* **2016**, *4*, 2432 – 2437; k) L. Tu, X. Liu, F. Wu, H. Zhang, *Chem. Soc. Rev.* **2015**, *44*, 1331 – 1345.

[6] a) F. Auzel, *Chem. Rev.* **2004**, *104*, 139 – 173; b) M. J. Weber, *Phys. Rev. B* **1971**, *4*, 2932 – 2939; c) W. J. C. Grant, *Phys. Rev. B* **1971**, *4*, 648 – 663.

[7] a) M. Y. Hossan, A. Hor, Q. Luu, S. J. Smith, P. S. May, M. T. Berry, *J. Phys. Chem. C* **2017**, *121*, 16592 – 16606; b) S. Alyatkin, I. Asharchuk, K. Khaydukov, A. Nechaev, O. Lebedev, Y. Vainer, V. Semchishen, E. Khaydukov, *Nanotechnology* **2017**, *28*, 035401; c) D. A. Zubenko, M. A. Noginov, V. A. Smirnov, I. A. Shcherbakov, *Phys. Rev. B* **1997**, *55*, 8881 – 8886; d) P. Villanueva-Delgado, K. W. Kraemer, R. Valiente, *J. Phys. Chem. C* **2015**, *119*, 23648 – 23657; e) S. Fischer, N. D. Bronstein, J. K. Swabeck, E. M. Chan, A. P. Alivisatos, *Nano Lett.* **2016**, *16*, 7241 – 7247.

[8] a) Q. Chen, X. Xie, B. Huang, L. Liang, S. Han, Z. Yi, Y. Wang, Y. Li, D. Fan, L. Huang, X. Liu, *Angew. Chem. Int. Ed.* **2017**, *56*, 7605 – 7609; *Angew. Chem.* **2017**, *129*, 7713 – 7717; b) D. J. Gargas, E. M. Chan, A. D. Ostrowski, S. Aloni, M. V. P. Altoe, E. S. Barnard, B. Sanii, J. J. Urban, D. J. Milliron, B. E. Cohen, P. J. Schuck, *Nat. Nanotechnol.* **2014**, *9*, 300 – 305; c) R. Deng, J. Wang, R. Chen, W. Huang, X. Liu, *J. Am. Chem. Soc.* **2016**, *138*, 15972 – 15979; d) D. Khoptyar, S. Sergeyev, B. Jaskorzynska, *J. Opt. Soc. Am. B* **2005**, *22*, 582 – 590; e) E. M. Chan, G. Han, J. D. Goldberg, D. J. Gargas, A. D. Ostrowski, P. J. Schuck, B. E. Cohen, D. J. Milliron, *Nano Lett.* **2012**, *12*, 3839 – 3845.

[9] J. Zhao, Z. Lu, Y. Yin, C. McRae, J. A. Piper, J. M. Dawes, D. Jin, E. M. Goldys, *Nanoscale* **2013**, *5*, 944 – 952.

[10] Y. Lu, J. Zhao, R. Zhang, Y. Liu, D. Liu, E. M. Goldys, X. Yang, P. Xi, A. Sunna, J. Lu, Y. Shi, R. C. Leif, Y. Huo, J. Shen, J. A. Piper, J. P. Robinson, D. Jin, *Nat. Photonics* **2014**, *8*, 33 – 37.

[11] a) W. Zheng, P. Huang, D. Tu, E. Ma, H. Zhu, X. Chen, *Chem. Soc. Rev.* **2015**, *44*, 1379 – 1415; b) R. B. Anderson, S. J. Smith, P. S. May, M. T. Berry, *J. Phys. Chem. Lett.* **2014**, *5*, 36 – 42.

[12] G. Chen, H. Qju, P. N. Prasad, X. Chen, *Chem. Rev.* **2014**, *114*, 5161 – 5214.

Manuscript received: November 13, 2017
Accepted manuscript online: January 24, 2018
Version of record online: February 14, 2018

